

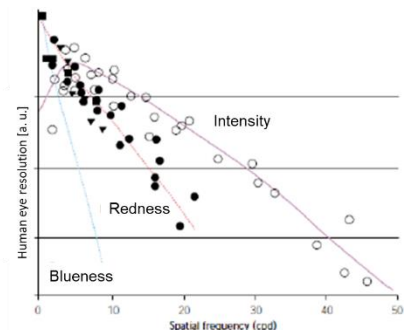
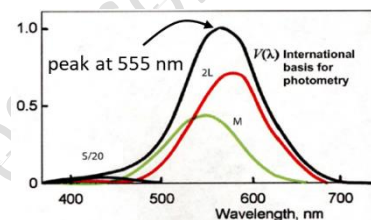
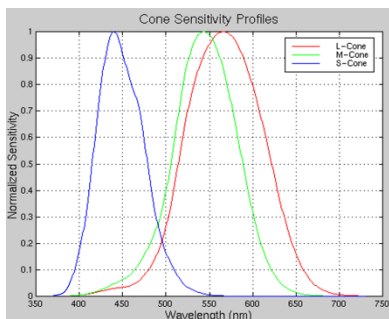
Question n. 1

After a brief discussion on how the human visual system generates color perception by our brain, describe the mostly used approach to get color images in digital cameras, its implementation, advantages, and drawbacks. Mention at least one alternative color capturing technique that you have studied in the course, with its advantages and drawbacks.

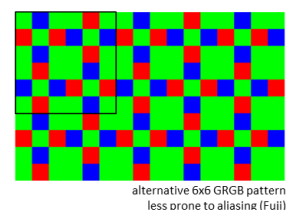
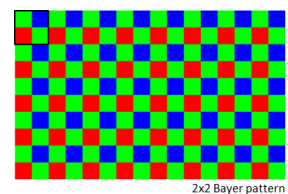
The human visual system generation of the color sensation is a combination of the different spectral sensitivity functions of the cones and the elaboration by the brain. More specifically, as each cone generates the same electrical stimulus to the optical nerve, the sensation of color depends on the relative weight of the number of photons captured by adjacent cones of different type. Two useful insights on these aspects are that:

- the overall (averaged) cones response, represented by the sum of the cones responses, weighted by their density in the fovea region, gives the photopic curve, i.e. the sensitivity function of the entire visual system to wavelengths. This curves peaks around 555 nm;
- the brain processing of cones stimuli rearranges the information from the three cones coordinates (LMS) into an intermediate color space in the brain which accounts for three channels: (i) brightness, (ii) yellowness/blueness and (iii) redness/greenness;
- the capability to discriminate details by the visual system depends much more on brightness than on the other two color channels.

The mentioned concepts are summarized by the images below.



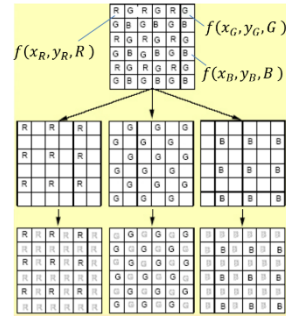
Most of digital imaging cameras try to mimic this working principle by using a spatial alternation of different color responses generated by microfilters (color filter arrays, CFA) deposited on top of the sensor. In the most common approach, there are three different spectral responses (RGB), just like for the human eye. Among RGB-type of CFA, the mostly adopted is then the so-called Bayer pattern, represented aside (top), where the green color channel is adopted twice with respect to blue and red channels. Small variations around this pattern can be implemented to make it less regular, so to minimize aliasing phenomena due to sampling at fixed spatial frequencies.



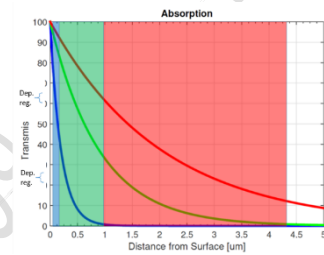
The reason why the green channel is used twice is 2-fold: (i) as it is the channel that mostly resembles the photopic curve, it gives a sensation of brightness comparable to the human eye and (ii) the capability to distinguish details in an image will be thus similar to a real scene, when seen by the human eye.

Despite the mentioned advantages, and the relatively low fabrication cost, CFAs imply also a few drawbacks:

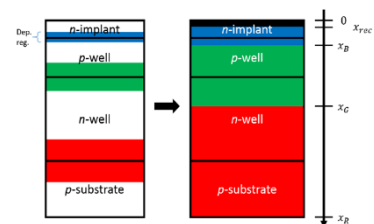
- from the process point of view, there is a need to deposit the CFA material, which in case of nonuniformities may lead to additional FPN contributions in terms of PRNU;
- from the computational effort point of view, the fact that the color channels are samples only each $\frac{1}{2}$ or $\frac{1}{4}$ of spatial position requires interpolation (so-called demosaicking, see the figure aside) to recover the full three-dimensional color information at each pixel position;
- the presence of filters generates a waste of light (and thus of signal) due to the absorption by the filter themselves.



One alternative approach to mitigate the effects above is the layered-junction sensor. This concept exploits the dependence of the absorption coefficient in Silicon on the wavelength: light in the blue range is indeed absorbed within few 100s nm, while light in the red range is fully absorbed only after several μm of thickness. Designing three layered, stacked, junctions at different depths allows capturing photoelectrons originating (mostly) from light of different spectral region, giving rise to three spectral functions of the impinging wavelength.



This is obtained without filter deposition. Additionally, the full 3-D color information is sampled at each pixel position without requiring interpolation (and associated computational cost or artifacts). Loss of light due to filters is also avoided, with consequent benefits in terms of SNR.



One issue of such pixels is the need for more complicated electronics, which does not lend well to ultra-compact pixels. For this reason, these innovative pixels have been so far mostly used in high-end cameras with pixel size of 6-8 μm , and not in mobile cameras where the pixel size should be as low as 1 μm .

MEMS & Microsensors

Question n. 2

A tuning-fork, mode-split, MEMS yaw gyroscope, with differential parallel plate sensing, features a drive loop based on a charge amplifier front-end, followed by gain and 90°-phase shifting stages, to satisfy the Barkhausen conditions. Other parameters of the system are reported in the table aside.

You are asked to:

- (i) find the maximum displacement of the drive frame, and the sensitivity (in [V/dps]) evaluated at the INA output;
- (ii) after writing the transfer function $Y(s)/F(s)$ of the sense mode, compute the phase shift (in [°]) between the Coriolis force and the sense displacement in such mode-split conditions. Quickly estimate, then, the phase error between the sense INA output and the demodulation reference, taken at the output of the 90°-shift stage (assume this latter stage ideal in terms of phase shift);
- (iii) how much does this phase error change over a temperature variation of +50 K?

Parameter [unit]	Value
Maximum linearity error	0.5 %
FSR [dps]	±2000
Process height [μm]	25
Drive resonance frequency [kHz]	20
Sense resonance frequency [kHz]	20.3
Process gap [μm]	1.5
Sense quality factor	800
Rotor voltage [V]	15
Drive and Sense feedback capacitor [pF]	0.5
Drive and Sense feedback resistor [G Ω]	10
Number of sense PP (half structure) N_{pp}	3
Length of each sense PP [μm]	200
Sense INA gain	1

Physical Constants

$$\epsilon_0 = 8.85 \cdot 10^{-12} \text{ F/m}$$

$$k_b = 1.38 \cdot 10^{-23} \text{ J/K;}$$

$$T = 300 \text{ K;}$$

$$q = 1.6 \cdot 10^{-19} \text{ C;}$$

(i)

We first check how the maximum displacement in the sensing direction is limited by linearity issues. By setting this condition, we find that:

$$y_{s,max} = 2000 \text{ dps} \cdot \frac{\pi}{180} \cdot \frac{x_d}{\Delta\omega} < \frac{1.5 \mu\text{m}}{10\sqrt{2}} \rightarrow x_d < 5.7 \mu\text{m}$$

The corresponding sensitivity value becomes:

$$S = 2 \frac{C_{S0} V_{Rot} x_d}{g C_{FS} \Delta\omega} G_{ina} = 2 \frac{\epsilon_0 h L_{pp} 2 N_{pp} V_{Rot} x_d}{g^2 C_{FS} \Delta\omega} G_{ina} \frac{\pi}{180} = 360 \frac{\mu\text{V}}{\text{dps}}$$

We note that for the FSR, the output voltage corresponds to $\pm 0.72 \text{ V}$ which is a reasonable value for an integrated circuit.

(ii)

The transfer function between the Coriolis force and the motion in the sensing direction is given by:

$$\frac{y_s}{F_{Cor}}(s) = \frac{1}{m_s} \frac{1}{s^2 + \frac{\omega_s}{Q_s} s + \omega_s^2}$$

As the Coriolis force acts around the drive frequency, the phase of this transfer function shall be evaluated for $s = j\omega_d$.

$$\frac{y_s}{F_{Cor}}(j\omega_d) = \frac{1}{m_s} \frac{1}{-\omega_d^2 + j \frac{\omega_s \omega_d}{Q_s} + \omega_s^2}$$

$$\phi \left[\frac{y_s}{F_{Cor}}(j\omega_d) \right] = \arctan \left(-\frac{\frac{\omega_s \omega_d}{Q_s}}{\omega_s^2 - \omega_d^2} \right) = \text{atan} \left(\frac{-\frac{f_d f_s}{Q_s}}{f_s^2 - f_d^2} \right)$$

As the term inside the brackets is small, we can approximate the arctangent with the angle. Additionally, we can write $f_d = f_s - \Delta f_{ds}$ to get:

$$\phi_s = \text{atan} \left(\frac{-\frac{f_d f_s}{Q_s}}{f_s^2 - f_d^2} \right) \approx \frac{-\frac{f_d f_s}{Q_s}}{f_s^2 - f_d^2} = \frac{-(f_s - \Delta f_{ds})f_s}{f_s^2 - (f_s - \Delta f_{ds})^2} = \frac{\frac{f_s \Delta f_{ds}}{Q_s} - \frac{f_s^2}{Q_s}}{-\Delta f_{ds}^2 + 2f_s \Delta f_{ds}}$$

Assuming then that Δf_{ds} is much smaller than f_s , we find a nice expression for the phase shift, which becomes:

$$\phi_s \approx \frac{-\frac{f_s^2}{Q_s}}{2f_s \Delta f_{ds}} = \frac{-f_s}{2\Delta f_{ds}} \frac{1}{Q_s} = \frac{Q_{eff}}{Q_s}$$

Which for the considered situation turns out to be -2.4° .

(iii)

The expression found above can be written as a function of temperature. To avoid losing the information on the drift of the resonance frequencies with temperature, we go back to the full form and add the temperature dependence through the coefficient α (-30 ppm/K).

$$\begin{aligned} \phi_s &= \frac{\frac{f_{s0}(1 + \alpha\Delta T)\Delta f_{ds0}(1 + \alpha\Delta T)}{Q_s(T)} - \frac{f_{s0}^2(1 + \alpha\Delta T)^2}{Q_s(T)}}{-\Delta f_{ds0}^2(1 + \alpha\Delta T)^2 + 2f_{s0}(1 + \alpha\Delta T)\Delta f_{ds0}(1 + \alpha\Delta T)} \\ \phi_s &= \frac{\frac{f_{s0}\Delta f_{ds0}(1 + \alpha\Delta T)^2}{Q_s(T)} - \frac{f_{s0}^2(1 + \alpha\Delta T)^2}{Q_s(T)}}{-\Delta f_{ds0}^2(1 + \alpha\Delta T)^2 + 2f_{s0}\Delta f_{ds0}(1 + \alpha\Delta T)^2} \\ \phi_s &= \frac{\frac{f_{s0}\Delta f_{ds0}}{Q_s(T)} - \frac{f_{s0}^2}{Q_s(T)}}{-\Delta f_{ds0}^2 + 2f_{s0}\Delta f_{ds0}} \approx \frac{-\frac{f_{s0}^2}{Q_s(T)}}{2f_{s0}\Delta f_{ds0}} = \frac{-f_{s0}}{2\Delta f_{ds0}} \frac{1}{Q_s(T)} = -\frac{Q_{eff0}}{Q_s(T)} \end{aligned}$$

We see that the dependence of the frequencies on temperature disappears, and we get again the same expression. Therefore, the only parameter that depends on temperature is the quality factor. It turns thus out that:

$$\frac{\delta\phi_s}{\phi_{s0}} = \frac{\delta Q_s(T)}{Q_{s0}} = -\frac{1}{2} \frac{\delta T}{T_0}$$

The change in phase and the new phase become thus:

$$\Delta\phi_s = \phi_{s0} \cdot \frac{\delta\phi_s}{\phi_{s0}} = 2.39^\circ \cdot 8.3\% = 0.2^\circ \rightarrow \phi_s(350\text{ K}) = 2.19^\circ$$

Last Name _MASCHE_

Given Name _RINA_

ID Number _20200910_

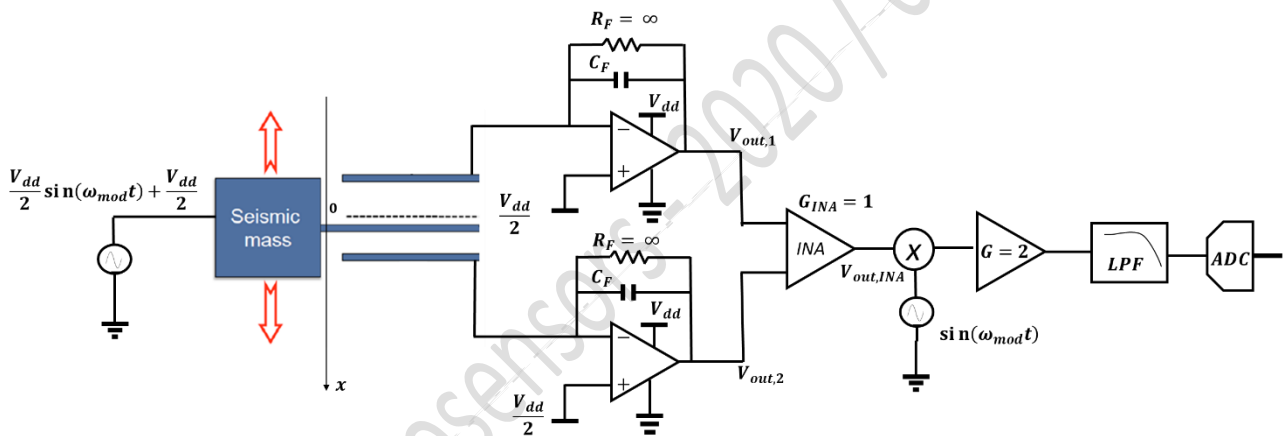
MEMS & Microsensors - 2020/09/10 - web

Question n. 3

The whole electronic readout chain of a parallel-plate MEMS accelerometer is reported below. Using the available data (see the Table aside), you are asked to:

Parameter [unit]	Value
Mechanical sensitivity (single ended) [fF/g]	2
Parasitic capacitance C_p [pF]	5
Operating temperature [K]	300
Input MOS overdrive voltage V_{ov} [V]	0.1
Mos γ coefficient	2/3
FSR [g]	± 16
Output low-pass-filter capacitance C_{LPF} [pF]	30
Output low-pass-filter resistance R_{LPF} [M Ω]	10
Supply voltage V_{dd} [V]	3.3
ADC number of bits	18

- (i) size the feedback capacitance of the charge-to-voltage amplifiers (assume zero offset);
- (ii) size the optimum polarization current of the input-pair transistors of the two operational amplifiers used for the C2V;
- (iii) consider now a mechanical offset corresponding to an input referred value of 5 g. Compute the output value of the ADC when no acceleration signal is present. Should you resize any components?
- (iv) with the same mechanical offset as above, and supposing that the feedback capacitance C_f changes over temperature with a coefficient of +30 ppm/K, calculate the input referred ZGO (zero-g offset) drift for a ΔT of +50 K.



Physical Constants
 $\epsilon_0 = 8.85 \cdot 10^{-12}$ F/m
 $k_b = 1.38 \cdot 10^{-23}$ J/K;
 $T = 300$ K;
 $q = 1.6 \cdot 10^{-19}$ C;

(i) The feedback capacitance of the charge amplifier should be sized in order to fully exploit the voltage dynamic at the INA output.

$$C_f = 2 S_{mech} FSR = 64 \text{ fF.}$$

(ii) The current of the OPAMP can be sized in order to have equal contribution to the total noise at the ADC input of the OPAMP and the maximum of the two noise sources in the circuit (no data are available to quantify the thermomechanical noise): the ADC and the RC low-pass filter.

The quantization noise results to be:

$$\sigma_q = \frac{LSB}{\sqrt{12}} = 3.6\mu V_{rms},$$

Instead the filter noise is:

$$\sigma_{LPF} = \sqrt{\frac{k_B T}{C_{lpf}}} = 11.7\mu V_{rms}.$$

Since the filter noise is greater than the quantization noise we should size the current as follows:

$$\sqrt{2S_{OPAMP} \left(1 + \frac{C_P}{C_F}\right)^2 BW} = \sigma_{LPF}$$

Where BW is the bandwidth set by the LPF, $BW = 1/2\pi R_{lpf} C_{lpf}$, and S_{OPAMP} the psd of the OPAMP of the charge amplifier. The factor 2 accounts for the noise of the two charge amplifiers.

The current turns out to be:

$$I = \frac{4k_B \gamma V_{ov}}{S_{OPAMP}} = 83\mu A.$$

(iii)

The input voltage of the adc when non acceleration is present and with an offset is:

$$V_{inADC} = \frac{V_{dd}}{2} + OS \cdot \frac{2S_{mech}V_{dd}}{2C_f}.$$

The transfer gain of the ADC (from input voltage to output number of levels) is:

$$G_{ADC} = \frac{2^{nbit}}{V_{dd}}.$$

Thus, the output of the ADC is:

$$\#_{outADC} = V_{inADC} G_{ADC} = 172032.$$

Since the feedback capacitance is sized in order to fully exploit the voltage range (0 - Vdd) at the INA output, the presence of a mechanical offset will cause a saturation of this stage. So the capacitance should be now sized in order to manage a full scale range of 21 g (16+5).

(iv)

If the capacitance changes of 30ppm/K, at 350K its value will be:

$$C_{f,350K} = C_f(1 + 30 \cdot 10^{-6} \cdot 50).$$

It is now possible to compute the output value of the ADC at 350K:

$$\#_{outADC,350K} = S_{350K} \cdot OS + 2^{nbit-1} = 171970.$$

And finally quote the input referred drift:

$$ZGO_{drift} = \frac{\#_{outADC,350K} - \#_{outADC}}{S} = 7.5mg.$$

MEMS & Microsensors - 2020/09/10 - web

